

Optical spectra beyond the amplifier bandwidth limitation in dispersion-managed mode-locked fiber lasers

Souad Chouli,^{1,*} José M. Soto-Crespo,² and Philippe Grelu¹

¹Laboratoire Interdisciplinaire Carnot de Bourgogne, UMR 5209 CNRS, Université de Bourgogne, 21000 Dijon, France

²Instituto de Óptica CSIC, Serrano 121, Madrid 28006, Spain

*souad.chouli@u-bourgogne.fr

Abstract: We investigate the intracavity pulse dynamics inside dispersion-managed mode-locked fiber lasers, and show numerically that for a relatively wide range of parameters, pulse compression dynamics in the passive anomalous fiber can be accompanied by a significant enhancement of the spectral width by a factor close to 3. Varying the average cavity dispersion also reveals chaotic dynamics for certain dispersion ranges. The impact of the implementation of an optical output port to tap optimal pulse features is discussed.

©2011 Optical Society of America

OCIS codes: (190.5530) Pulse propagation and temporal solitons; (140.4050) Mode-locked lasers; (140.3510) Lasers, fiber.

References and links

1. K. Tamura, E. P. Ippen, H. A. Haus, and L. E. Nelson, "77-fs pulse generation from a stretched-pulse mode-locked all-fiber ring laser," *Opt. Lett.* **18**(13), 1080–1082 (1993).
2. F. M. Knox, W. Forysiak, and N. Doran, "10-Gbit/s soliton communication systems over standard fiber at 1.55 μm and the use of dispersion compensation," *J. Lightwave Technol.* **13**(10), 1955–1962 (1995).
3. H. A. Haus, K. Tamura, L. E. Nelson, and E. P. Ippen, "Stretched-pulse additive pulse mode-locking in fiber ring lasers: theory and experiments," *IEEE J. Quantum Electron.* **31**(3), 591–598 (1995).
4. I. Gabitov, E. G. Shapiro, and S. K. Turitsyn, "Optical pulse dynamics in fiber links with dispersion compensation," *Opt. Commun.* **134**(1-6), 317–329 (1997).
5. B. G. Bale, S. Boscolo, J. N. Kutz, and S. K. Turitsyn, "Intracavity dynamics in high-power mode-locked fiber lasers," *Phys. Rev. A* **81**(3), 033828 (2010).
6. Ph. Grelu, J. Béal, and J. M. Soto-Crespo, "Soliton pairs in a fiber laser: from anomalous to normal average dispersion regime," *Opt. Express* **11**(18), 2238–2243 (2003).
7. J. M. Soto-Crespo, M. Grapinet, Ph. Grelu, and N. Akhmediev, "Bifurcations and multiple-period soliton pulsations in a passively mode-locked fiber laser," *Phys. Rev. E Stat. Nonlin. Soft Matter Phys.* **70**(6), 066612 (2004).
8. S. Chouli, and Ph. Grelu, "Rains of solitons in a fiber laser," *Opt. Express* **17**(14), 11776–11781 (2009).
9. H. A. Haus, "Mode-locking of lasers," *IEEE J. Sel. Top. Quantum Opt.* **6**(6), 1173–1185 (2000).
10. G. P. Agrawal, *Nonlinear Fiber Optics* 4th Edition. (Academic Press, Boston 2007).
11. K. C. Chan, H. F. Liu, K. C. Chan, and H. F. Liu, "Short pulse generation by higher order soliton-effect compression: effects of optical fiber characteristics," *IEEE J. Quantum Electron.* **31**(12), 2226–2235 (1995).

1. Introduction

The implementation of dispersion-management in mode-locked fiber lasers has allowed an important increase of pulse energy, and offered a particularly useful degree of freedom in the cavity design [1]. Due to the large local dispersion and low path-averaged dispersion, the mode-locked pulse propagates stretched in most part of the cavity, while its temporal duration undergoes a significant breathing in both anomalously and normally dispersive fiber links. Dispersion management has also become familiar to the field of optical transmission as a powerful scheme for suppression of the Gordon-Haus timing jitter, as well as to reduce nonlinearity impairments [2]. Since then, numerous studies of stretched-pulse dynamics have been undertaken [3–5]. Besides the interesting power scaling from conventional-soliton based fiber lasers [3], original single-pulse and multi-pulse dynamics have been found in dispersion-

managed mode-locked fiber lasers, and have been interpreted in the frame of the dissipative soliton concept [6–8]. Although single-pulse dynamics in dispersion-managed fiber laser cavities have been largely investigated, we have observed numerically the following significant effects that have not yet been reported, to our knowledge. The main point consists in the large magnitude of the spectral breathing effect – an effect which has mostly gone unnoticed so far- in specific dispersion-managed cavity designs. The possible use of this spectral breathing effect as a way to output a pulse with an optical bandwidth exceeding that of the amplifying medium is discussed. In the course of optimizing this effect through dispersion management, the existence of dispersion gaps where no stable mode locking can be obtained - unless other cavity parameters are altered- is reported. Finally, we discuss the implementation of an output laser port to tap the pulse at its maximal bandwidth.

2. Spectral breathing from a dispersion-managed fiber laser model

As in the original works of Ref.1 on dispersion-managed fiber lasers, the cavity design includes an erbium-doped gain fiber with normal dispersion (EDF), a passive fiber of anomalous dispersion (SMF), and an ultrafast saturable absorber (SA). In order to decouple the setting of the path-averaged dispersion from that of the gain medium, we included a dispersion-compensation fiber (DCF), whose moderate length could be conveniently changed. Successive cavity elements are shown in Fig. 1.



Fig. 1. Schematic of the fiber laser cavity

Effective losses for the saturable absorber and the output coupler elements have been included. We have considered the following scalar propagation model taking account discrete elements. In the passive fibers (SMF, DCF), the propagation of the electric field envelope $E(t, z)$ along the distance z is computed using the nonlinear Schrödinger equation:

$$i E_z + \frac{D_k}{2} E_{tt} + \Gamma_k |E|^2 E = 0, \quad (1)$$

where D_k is the dispersion parameter, and Γ_k the nonlinear coefficient of the fiber referred to by the index k ($k = \text{SMF, DCF, or EDF}$). In the EDF, field propagation is modeled by:

$$i E_z + \frac{D_k}{2} E_{tt} + \Gamma_k |E|^2 E = \frac{i g_0 / 2}{1 + Q(z) / Q_{sat}} \left(1 + \frac{\partial_{tt}^2}{\Omega_g^2} \right) E, \quad (2)$$

where $Q(z) = \int_{-\infty}^{+\infty} |E(t, z)|^2 dt$ represents the total field energy at distance z , Q_{sat} is the saturation energy that is proportional to the pumping power, g_0 is the small signal gain fixed by the erbium concentration in the EDF, and the gain bandwidth is Ω_g . The instantaneous saturable absorber (SA) is modeled by the following generic nonlinear transfer function [9]:

$$T = T_0 + \Delta T \frac{I(t)}{P_{sat} + I(t)}, \quad (3)$$

with $I(t) = |E(t)|^2$, T_0 , ΔT and P_{sat} stand for the low transmission level, the transmission contrast, and the saturation power, respectively. The main output coupler is placed after the saturable absorber. The intrinsic nonlinearity of silica $n_2 = 2.5 \cdot 10^{-20} \text{ m}^2 \cdot \text{W}^{-1}$ is assumed for all fibers, from which the nonlinear coefficients Γ_k are calculated taking into account the mode field areas.

We have initially considered the following fiber parameters that are typical of commercially available fibers:

- Gain medium: $D_{EDF} = -12.5 \text{ ps.nm}^{-1}.\text{km}^{-1}$; mode field area $A_{EDF} = 28.3 \text{ }\mu\text{m}^2$; $L_{EDF} = 2.2 \text{ m}$; $g_0 = 1.3\text{m}^{-1}$; and $\Omega = 3.12 \text{ THz}$ corresponding to $\Delta\lambda = 25 \text{ nm}$;
- Passive fiber: $D_{SMF} = +17 \text{ ps.nm}^{-1}.\text{km}^{-1}$; $A_{SMF} = 78.5 \text{ }\mu\text{m}^2$; $L_{SMF} = 10.4\text{m}$;
- Dispersion compensation fiber: $D_{DCF} = -91 \text{ ps.nm}^{-1}.\text{km}^{-1}$; $A_{DCF} = 28.3 \text{ }\mu\text{m}^2$; $L_{DCF} = 1.6 \text{ m}$ is used to obtain an average cavity dispersion close to zero: $D_{ave} = 0.26 \text{ ps.nm}^{-1}.\text{km}^{-1}$.

For the saturable absorber, a large modulation is used as in design of the majority of mode-locked fiber lasers: $T_0 = 0.70$, $\Delta T = 0.30$, and $P_{sat} = 10\text{W}$. Effective losses (OC) amount to 86%.

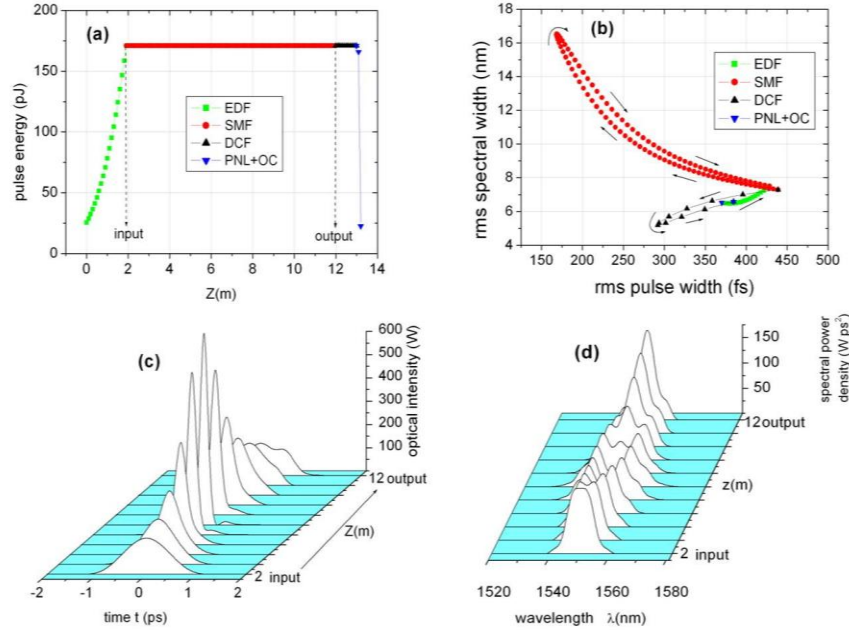


Fig. 2. Illustration of stable mode locking with large spectral breathing: (a) changes in the pulse energy Q within one cavity roundtrip, (b) changes in pulse duration and spectral width, and (c) temporal breathing and (d) spectral breathing inside of the passive fiber (SMF) section. We used $Q_{sat} = 200 \text{ pJ}$.

For a sufficient gain level, an initial white temporal noise can evolve into a stable mode-locked regime. Then, as the pulse propagates through the different sections of the laser cavity, its energy evolves as in Fig. 2(a). Typical of dispersion-managed cavity dynamics, the pulse temporal width undergoes a large breathing during each roundtrip, as illustrated by Fig. 2(b) and (c). In addition, it is surprising to see, in Fig. 2(b) and (d), the large magnitude of the spectral breathing effect, with a spectral breathing ratio of 2.5. For a large domain of system parameters, the spectral width is broadened by a factor comprised between 2 and 3 during propagation inside the passive anomalous-dispersion fiber. Spectral broadening in the SMF can be understood as follows: after leaving the normal gain medium, the amplified pulse enters the SMF with an up-chirp, which entails temporal compression in the anomalous medium. Along with compression, self-phase modulation (SPM) is enhanced, producing extra frequency components that lead to an increase of temporal compression. The location of the minimal pulse duration and that of the maximal spectral width do not always coincide, but are located close to each other. A little farther in the SMF, the pulse becomes down-chirped: its side spectral components move away from the center of the pulse, where they meet an opposite frequency shift from SPM, hence the subsequent reduction of the spectral width of the pulse, as seen in the second part of the red curve in Fig. 2(b). After the SMF, dispersion

management with the DCF reverses the evolution of pulse duration. However, this does not apply in the spectral domain: SPM further reduces the spectral width in the DCF as long as the pulse remains up-chirped. Then, after experiencing a significant amount of losses (saturable absorber, output coupler, splices) the pulse enters the normally dispersive gain fiber with a moderate up-chirp. Note that, since spectral and temporal distortions are important during spectral breathing, we have used full RMS widths instead of FWHM. For a Gaussian spectrum, the FWHM amounts to $(2 \ln 2)^{1/2}$ times the full RMS width, but naturally the relationship between the two is highly dependent on the spectral profile.

Spectral broadening due to self-phase modulation is a well-known effect that has also been used in high-order soliton compression schemes for instance [10,11]. However, a potentially large spectral broadening effect has not yet been identified in dispersion-managed fiber laser cavities. It is interesting to notice that the above laser cavity design offers the potential of delivering ultrashort pulses with a spectral content exceeding the amplifier bandwidth limitations, provided that one can output the pulse close to its minimum duration. As exceeding the amplifier bandwidth is clearly not the situation depicted in Fig. 2, we explain in the following section how cavity rescaling can be used to optimize some of the pulse dynamical features.

3. Cavity scaling

It is worth recalling how pulse features are affected by cavity scaling. If the dimension of the cavity is scaled down by a factor $K < 1$, namely $Z' = KZ$, and considering the same amount of losses, a scaled dynamics can be found provided that the total gain remains constant, $g_0' = K^{-1}g_0$, and that the gain bandwidth is increased such as $\Delta\Omega' = K^{-1/2}\Delta\Omega$. In that case, the scaled-down cavity features the *same dynamics* with shorter time scales $T' = K^{1/2}T$, increased spectral widths $\Delta\lambda' = K^{-1/2}\Delta\lambda$, increased power scales $P' = K^{-1}P$ and energy scales $E' = K^{-1/2}E$. The saturation intensity P_{sat} and the saturation energy Q_{sat} should be changed accordingly. However in practice, although the fiber lengths, the concentration of active ions and the saturable absorber design can be widely changed, the gain bandwidth is bound to the spectroscopic properties of the gain material. Hence in the following, we applied the scaling factor K to all of the above-mentioned variables *except* the gain bandwidth that was kept constant (25 nm). With a fixed gain bandwidth, *similar but not identical spectral-breathing dynamics can be obtained through realistic cavity downscaling*. This way, cavity downscaling provides a way to obtain a pulse spectral width in the passive fiber that becomes larger than the amplifier bandwidth. Figure 3 is an illustration of this feature: from $K = 1$ to $K = 0.25$, the maximum spectral width increases from 16.3 to 32.5 nm, above the amplifier bandwidth (25 nm), and the minimal temporal width is reduced from 170 to 90 fs. Ultimately, there are also practical limits in terms of the doping concentration of the gain fiber, and the shortness of fiber links that can be used. Based on existing EDFs, a lower boundary for K around 0.1 is a reasonable figure.

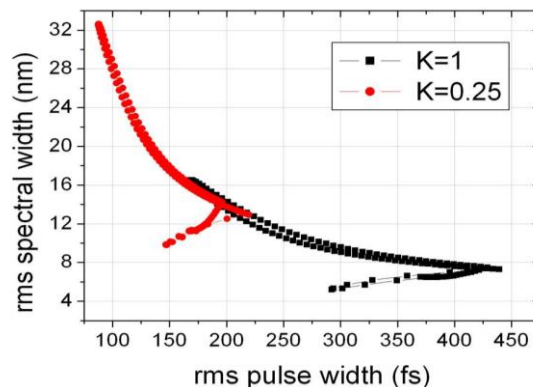


Fig. 3. spectro-temporal pulse breathing for initial cavity parameters ($K = 1$, black curve) and after cavity downscaling by a factor of 4 ($K = 0.25$, red curve).

4. Gaps in the tuning of the average dispersion

Varying the gain of the EDF and the length of the DCF, we obtain a significant spectral breathing effect for an averaged chromatic dispersion lying between -2 and $+6$ ps.nm $^{-1}$.km $^{-1}$, with a maximum close to zero path-averaged dispersion and a RMS spectral width enhancement up to 3.24 inside of the SMF. However, we found that, in general, we cannot maintain stable mode locking through continuously varying the DCF length: there are dispersion gaps where pulses are not stable, as illustrated by Fig. 4. This is particularly true for large-gain or, equivalently, highly-pumped EDF.

Figure 4 is obtained as follows: starting without dispersion compensation fiber ($L_{DCF} = 0$), we propagate any arbitrary input pulse until reaching a given solution. Then, L_{DCF} is increased, and as a new initial condition we take the solution of the previous step. After removing any transitory behavior, the values of the energy (Q) of the output pulses for the next 100 roundtrips are represented by small dots. When there is a single stationary solution, all dots coincide. Period-N solutions are represented by N distinct points and so on. The process is repeated until scanning completely the desired interval of values of L_{DCF} [7]. The three differently colored curves correspond to three different values of the small signal gain. The green curve, for the smallest g_0 , mostly shows the existence of a single stationary pulse until $L_{DCF} = 1.85$ m. Then, a very wide low amplitude pulse is obtained. When increasing the small signal gain this upper limit occurs at higher L_{DCF} values, namely 1.94 and 2 m for the blue and red curves respectively. When the energy pumped into the system gets higher, the complexity of the dynamics increases. Single stationary pulses are obtained for smaller intervals of values of L_{DCF} . Period-2 solutions, periodic solutions with periods much larger than the roundtrip, even incommensurate with it, and chaotic pulses can be observed.

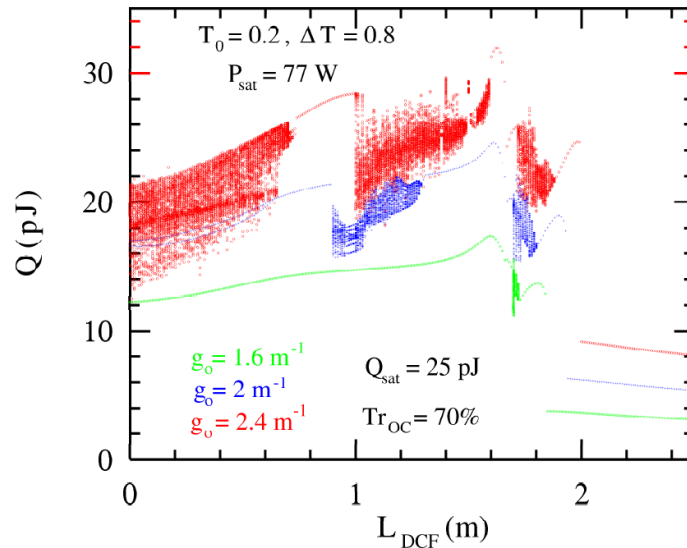


Fig. 4. Output energy versus the dispersion-compensation fiber (L_{DCF}), for various gain values g_0 . Mode locking gaps can be clearly seen in all cases, being wider and more frequent as the energy pumped into the system increases. The values of the parameters that are different from those used in Fig. 2 are written inside the figure.

5. Optical tapping an optimal output pulse

The implementation of an optical coupler at the location where the spectral width is maximal, close to the middle of the SMF segment, affects the overall dynamics. For instance, it has not been possible to merely shift the main optical coupler that is located after the saturable absorber and put it in the middle of the SMF: the spectral breathing dynamics then disappears. The existence of important losses right before entering the gain section seems a prerequisite to

maintaining the spectral breathing dynamics. Thus, we have kept the main output coupler and included another output coupler close to the middle of the SMF, with a moderate coupling ratio of 10%. This way, the spectral breathing dynamics is preserved, with a broadening factor close to 3. Discussing the extraction of an optimized pulse, we have to take into account the spectral distortion arising from SPM, which can lead to multi-peaks on the sides and to a large dip in the center of the spectrum. Spectral distortion strongly depends on the pulse intensity, as well as on the initial frequency chirp [9]. Limiting the saturation energy – which grows proportionally to the pumping power – to moderate values allows maintaining the spectral profile rather smooth. The strong influence of the saturation energy is illustrated in Fig. 5, which plots the pulse spectral and temporal features obtained in the middle of the SMF segment through a 10%-coupler for the following values Q_{sat} : 400, 500 and 650 pJ. We used $K = 0.36$ in these examples, and one can see that maximal spectral width is obtained at the expense of the pulse shape.

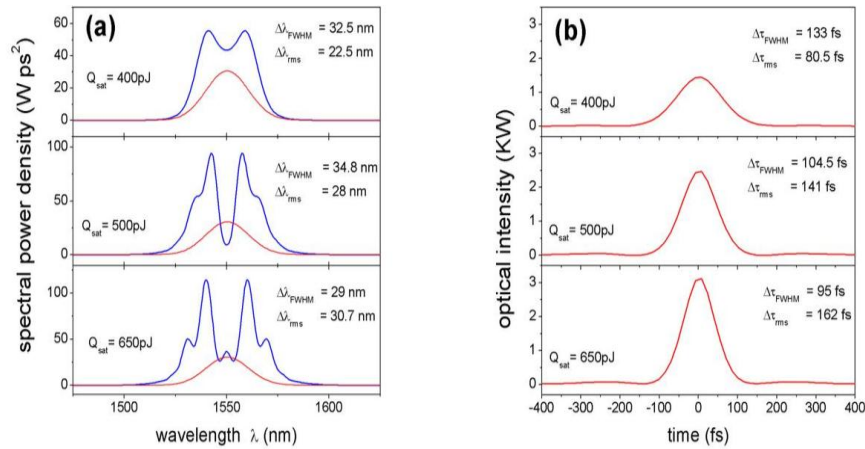


Fig. 5. (a) optical spectra (in blue) at the additional 10%-output coupler located in the middle of the SMF, for different values of the saturation energy Q_{sat} . The gain spectral profile is assumed to be a 25-nm wide Gaussian function (in red). (b): corresponding pulse intensity profiles.

6. Summary and conclusion

In dispersion-managed mode-locked fiber lasers, we have found that the well-known temporal breathing effect can be accompanied by a large spectral breathing effect as well. This spectral breathing effect has the potential to produce, in a localized segment midway of the passive anomalous fiber, a pulse whose bandwidth exceeds well the amplifier bandwidth. Such dynamics manifests when there are large losses – typically 80% - per round trip, localized before the amplifier segment, and is prominent in a fiber laser setup that includes a normally-dispersive passive fiber link – DCF – before the amplifier. The optimum of spectral breathing is obtained close to the zero path-averaged chromatic dispersion. Besides this remarkable spectral dynamics, we have addressed the question of its potential use in fiber laser experiments. First, to achieve a pulse whose bandwidth exceeds the amplifier bandwidth, a correct cavity scaling needs to be performed. Second, to output the pulse at its minimal duration and maximal spectral width, power tapping with a moderate output-coupling ratio should be performed. Third, spectral distortion affects the pulse, and increase along with the pumping power. Although these conditions could make the scheme rather inconvenient for practical applications, considering the large number of degrees of freedom, it is likely that spectral breathing can be further optimized, or found in a very different fiber laser setup.

Acknowledgements

S.C. acknowledges financial support from Conseil Régional de Bourgogne and from Université de Bourgogne. J.M.S.C. acknowledges support from the Spanish Ministerio de Ciencia e Innovación under contracts FIS2006-03376 and FIS2009-09895.